

HOBr in Sulfuric Acid Solutions: Solubility and Reaction with HCl as a Function of Temperature and Concentration

Gabriela C. G. Waschewsky and Jonathan P. D. Abbatt*

Department of the Geophysical Sciences, The University of Chicago, Chicago, Illinois 60637

Received: November 19, 1998; In Final Form: May 4, 1999

A detailed study of the interaction of HOBr and HCl in cold sulfuric acid solutions has been performed using a coated-wall flow tube coupled to an electron-impact mass spectrometer. The liquid-phase bimolecular rate constants, measured over a temperature range from 213 to 238 K and in solutions from 59.7 to 70.1 wt % composition, show a strong positive dependence on both acid composition and temperature. The solubility of HOBr has also been measured in these solutions by analyzing its time-dependent uptake. Henry's Law constants (H) determined from the measured values of $HD^{1/2}$ and the liquid-phase diffusion coefficient (D) are independent of acid composition over the above range of solution compositions. The values of H demonstrate a clear Clausius–Clapeyron temperature dependence, with a heat of solution of -9 ± 1 kcal/mol. When the atmospheric importance of these data is assessed, two conclusions are reached. In the stratosphere, under aerosol conditions observed soon after the Mt. Pinatubo volcanic eruption, the rates of HCl activation via the HOBr/HCl heterogeneous reaction are comparable with the rate of activation via gas-phase reaction with OH at relatively warm temperatures (205–220 K), where other HCl-activating heterogeneous reactions occur slowly. In the high Arctic boundary layer, it is possible that significant HCl activation could occur when elevated levels of photochemically active bromine are present.

Introduction

Although the total atmospheric loading of inorganic bromine is relatively low, not exceeding a few tens of parts per trillion,¹ there has been considerable interest in recent years in the heterogeneous interactions which brominated species undergo in the atmosphere. This interest has arisen because a number of reactions involving bromine species proceed at very high rates, in some cases many orders of magnitude larger than the corresponding reactions involving chlorine. From the perspective of the stratosphere, the two reactions which have been identified as being of most importance are (R1) and (R2), when they occur on sulfate aerosols:

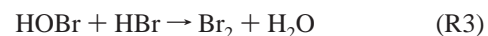


The first is thought to proceed very efficiently, with a reaction probability approaching unity. The process is of considerable importance as both a HO_x source, via the photolysis of the HOBr product, and a NO_x sink.² On the other hand, (R2) has the potential to be of significance in directly activating HCl.^{2,3} At the low temperatures encountered at high latitudes in winter and springtime, stratospheric sulfate aerosols become dilute and the solubility of both HOBr and HCl is high, leading to an efficient condensed phase reaction. Two preliminary studies, one from our laboratory and one from that of Hanson and Ravishankara, have indicated that the reaction proceeds sufficiently rapidly that it needs to be considered when assessing the rates of HCl activation at low temperatures in the stratosphere.^{2,3}

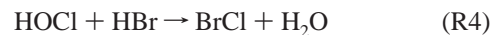
From the perspective of the troposphere, there is growing evidence that hydrogen halides such as HCl and HBr can be activated in much the same manner by which they are activated

in the cold stratosphere. In the troposphere, high relative humidities can create sulfate aerosols which are considerably more dilute than their counterparts in the stratosphere, thus enhancing the solubility of species such as HCl, HBr, HOCl, and HOBr, and increasing the rates of condensed phase reactions. This set of conditions is frequently encountered, for example, in the springtime Arctic boundary layer where the relative humidity is close to saturation with respect to ice and temperatures can reach many tens of degrees below freezing.

Evidence for activation of halogen species in the high Arctic is now well established. Bromine is activated in the springtime boundary layer.^{4,5} Similarly, high levels of active chlorine have been both measured directly, and inferred from enhanced loss rates of hydrocarbons.⁵ Although there is considerable uncertainty concerning the original sources of both the active bromine and chlorine, it is now believed that recycling of active halogens via HOX/HY reactions, where X and Y are halogens, contributes to their high levels. For example, for the activation of HBr, Fan and Jacob modeled that the reaction of HOBr with HBr on sulfate aerosols:

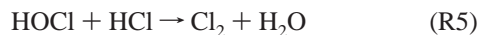


could readily maintain high levels of active bromine, assuming a realistic estimate for the kinetics of the reaction.⁶ Recently, we have suggested that the reaction



may also be important at activating HBr, given that high levels of photochemically active chlorine may also be present.⁷ Indeed, based on the first laboratory kinetics studies performed in sulfuric acid, estimates of the rates of HBr activation via these two reactions suggest that both could proceed sufficiently rapidly

to maintain high levels of active bromine during the Arctic spring.⁷ For the activation of HCl, the two most likely recycling processes are expected to occur via interactions with HOBr (R2) and HOCl (R5):



An additional motivation to the study of the HOX/HY reactions comes from models of the interactions of HOBr with sea salt aerosols in both polluted and pristine environments at mid-latitudes. It has been suggested that the interaction of HOBr with marine aerosols may lead to an autocatalytic release of bromine from the aerosol.^{8–10} The full impact of this chemistry, which includes sizable ozone destruction and S(IV) oxidation, is dependent upon both the rate of HOBr uptake by sea salt aerosols and the extent of the recycling of halogens through heterogeneous processes occurring with marine sulfate aerosols.

Motivated by the atmospheric importance of HCl activation processes, we have performed a detailed experimental study of the kinetics of (R2) in cold sulfuric acid solutions. As mentioned above, two previous studies have measured similar, fast kinetics for the reaction.^{2,3} However, the sets of conditions under which these experiments were conducted were quite limited: in our work, the reaction was studied in 70 wt % acid at 228 K, and in the work of Hanson and Ravishankara, the reaction was studied in 60% acid at 210 K. In the present study, we perform measurements over a much wider range of both temperatures (from 213 to 238 K) and acid compositions (from 59.7 to 70.1 wt %), with the goal being to formulate a parametrization of the rate of the reaction which can be used under a range of atmospheric conditions. We have also performed a study of the time-resolved uptake of HOBr by sulfuric acid solutions, in order that its solubility in these solutions can be determined. We have performed these kinetics experiments in a manner which we believe to be more appropriate than that performed in the two earlier studies, and the general conclusions are that this reaction proceeds substantially faster under atmospheric conditions than was previously thought.

Experimental Section

We used a low-temperature flow tube coupled to a mass spectrometer to measure (1) the time-dependent, reversible dissolution of HOBr into cold sulfuric acid solutions, and (2) the steady-state loss due to liquid-phase reaction of HCl with HOBr dissolved in a sulfuric acid solution. For both sets of experiments, the active surfaces were prepared by coating the clean inner walls of a 2.34-cm-i.d. Pyrex tube with sulfuric acid solution, as described previously.^{3,7} The coated reaction tube was then carefully inserted into the cooled region of a horizontal flow tube; the flow tube was sealed and the sulfuric acid film was allowed to reach thermal equilibrium with the flow tube. At the low temperatures used, the sulfuric acid solutions were viscous enough to coat the walls over the course of each measurement. The sulfuric acid films remained liquid under all conditions of the experiment. To ensure unchanging acid composition over the duration of each measurement, water vapor was added to the flow tube by bubbling a small flow of He through a water trap. Water partial pressures were adjusted to match within 10% the water vapor pressure of the sulfuric acid film at the temperature of the experiment.¹¹ An electron-impact mass spectrometer was used to monitor the composition of the gas phase in the flow tube, with detection limits (S/N = 1, integration times of 1 s) of 3×10^{-10} atm for HCl, and 5×10^{-11} atm for both BrCl and HOBr.

The time-dependent measurements were taken by first establishing a flow of HOBr through a movable injector which was pushed into the flow tube fully past the end of the sulfuric acid film. Average HOBr partial pressure in the flow tube was $\sim 5 \times 10^{-10}$ atm. When a steady mass spectrometer signal was achieved, the injector was quickly pulled back a few centimeters, exposing the film to the HOBr. This action results in an immediate initial drop in the HOBr signal as the HOBr is taken up by the sulfuric acid solution, followed by a recovery of the signal as saturation starts to occur. At some time later, the injector is pushed back in to its original position, producing a surge in the HOBr signal as the dissolved HOBr desorbs.

The time-dependent data were analyzed as in earlier studies.^{3,7} At each point in time, t , a net uptake coefficient is calculated from the initial HOBr signal and the signal at time t . To correct for radial concentration gradients in the flow tube, the calculation includes the gas-phase diffusion correction described in Brown.¹² The time-dependent uptake of a gas into an infinitely thick liquid which initially contains no dissolved gas¹³ is described by (E1):

$$\gamma(t) = 4RTHD^{1/2}/c(\pi t)^{1/2} \quad (\text{E1})$$

where $\gamma(t)$ is the time-dependent uptake coefficient, R is the ideal gas constant, T is the temperature, c is the mean gas velocity, and H and D are the Henry's law coefficient and liquid-phase diffusion coefficient, respectively, for HOBr in sulfuric acid. The set of time-dependent uptake coefficients calculated from the data are plotted versus $t^{-1/2}$ to yield a straight line in accord with (E1), assuming that the mass accommodation coefficient for HOBr is close to unity, as has been shown to be the case for HOCl.¹⁴

For the reactive uptake experiments, a small amount of HCl was entrained in He to flow through the movable injector, while HOBr was introduced into the upstream end of the reaction flow tube, at partial pressures sufficient to ensure HOBr would be well in excess over HCl in solution. P^{HOBr} ranged from 9×10^{-10} to 1×10^{-7} atm, with typical P^{HCl} at 2×10^{-10} to 9×10^{-10} atm, and $[\text{HOBr}]/[\text{HCl}]$ varied from 30 to 3×10^5 in the liquid phase. The first-order loss of HCl, or growth of BrCl, was monitored as a function of distance as the injector was pulled back through the flow tube. In the absence of radial concentration gradients in the flow tube, the probability for reactive loss of HCl to the wall, γ^{HCl} , is directly proportional to the first-order rate constant. At high wall-loss rates, diffusion through the buffer gas to the wall restricts the overall loss rates, and a diffusion correction is applied to the observed data. The diffusion coefficient used in this calculation was $0.105 T^{3/2}/P$ cm²/s for HCl, with P in Torr and T in Kelvin. Typical flow tube pressure was 1 Torr He. The HOBr partial pressure was monitored at the start and finish of each kinetics experiment to correct for any drift in the HOBr source.

The steady-state reaction probability for HCl being lost from the gas phase through a pseudo first-order reaction in the liquid is described by¹³

$$1/\gamma^{\text{HCl}} = 1/\alpha + c/4RTH^{\text{HCl}}(D^{\text{HCl}}k^{\text{l}})^{1/2} \quad (\text{E2})$$

$$\gamma^{\text{HCl}} \approx 4RTH^{\text{HCl}}(D^{\text{HCl}}k^{\text{l}})^{1/2}/c \quad (\text{E3})$$

where k^{l} is the first-order liquid-phase rate constant and α is the mass accommodation coefficient. The approximation in (E3) is valid for $\gamma^{\text{HCl}} \leq 0.2$, if $\alpha \approx 1$. For pseudo first-order kinetics, $k^{\text{l}} = k^{\text{II}}[\text{HOBr}]$, where k^{II} is the second-order liquid-phase rate constant and $[\text{HOBr}]$ is the liquid-phase concentration of HOBr. With $[\text{HOBr}] = H^{\text{HOBr}} P^{\text{HOBr}}$, (E2) and (E3) may be rewritten

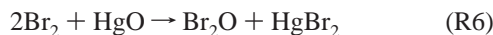
as

$$1/\gamma^{\text{HCl}} = 1/\alpha + c/4RTH^{\text{HCl}}(D^{\text{HCl}}k^{\text{II}}H^{\text{HOBr}}P^{\text{HOBr}})^{1/2} \quad (\text{E4})$$

$$\gamma^{\text{HCl}} \approx 4RTH^{\text{HCl}}(D^{\text{HCl}}k^{\text{II}}H^{\text{HOBr}}P^{\text{HOBr}})^{1/2}/c \quad (\text{E5})$$

respectively.

To generate a continuous supply of HOBr, a steady-state flow of Br₂ was passed through a 1-cm-i.d., 60-cm-long glass tube loosely packed with a mixture of yellow mercuric oxide and 2 mm glass beads.¹⁵ The bromine was entrained in a 90 sccm flow of He, a portion (~12 sccm) of which was bubbled through a water trap. The bromine reacts with the mercuric oxide to form Br₂O, which is converted to HOBr upon reaction with water:



Coupling the mass spectrometer to an absorption cell, as described below, allowed us to calibrate the mass spectrometer signal for HOBr to the partial pressure in the flow tube, and to measure the conversion efficiency of the HOBr source. About five percent of the Br₂ entering the HgO tube is converted to HOBr. The conversion efficiency varied with relative humidity (RH): 10 to 20% was optimum under our conditions, which were typically 150–200 Torr and 295 K. At higher RH, the bromine would be lost, perhaps to reaction with metal fittings in our system; at lower RH, the equilibrium in reaction (R7) would shift to the left. The amount of residual Br₂O, as monitored by mass spectrometry, was reduced by maintaining the highest RH the experiment would allow, or else, by operating at very low concentrations of HOBr. After a brief conditioning period, the supply of HOBr was relatively constant in time.

The absorption cell used to calibrate the partial pressure of HOBr in the flow tube was connected just upstream of the flow tube. We measured P^{HOBr} in the cell by directing the 254 nm line from a mercury lamp down the length of the cell and through an interference filter, and collecting the transmitted light with a photodiode:

$$P = -RT \ln(I/I_0)/\sigma l N_A \quad (\text{E6})$$

where *I* is the intensity of light transmitted by the absorber, *I*₀ is the intensity in the absence of the absorber, σ is the absorption cross section for HOBr at 254 nm,¹⁶ *l* is the length of the tube (50 cm), and *N*_A is Avogadro's number. Since bromine has a nonnegligible absorption cross-section at 254 nm, we connected a bypass valve around the mercuric oxide tube to measure an *I*₀ that accounts for the bromine in the absorption cell. The low conversion efficiency (5%) means that the change in *I*₀, when the bromine is directed through the mercuric oxide tube instead of around it, contributes only about 10% uncertainty in the HOBr partial pressures. Together with the uncertainty in the cross section, we estimate uncertainties of ±20% in the HOBr partial pressure measurements by this technique.

Br₂O also has a substantial cross-section at 254 nm.¹⁶ We therefore monitored the system closely for evidence of its presence. At total absorption cell pressures greater than 200 Torr, with high partial pressures of HOBr, we saw evidence for Br₂O contamination in the form of a small mass spectrometer signal at the parent mass, which disappeared when the room lights were turned on, and as a nonlinear increase in the ratio of absorbance to mass spectrometer signal. To minimize this contribution, we made all absorbance measurements at total

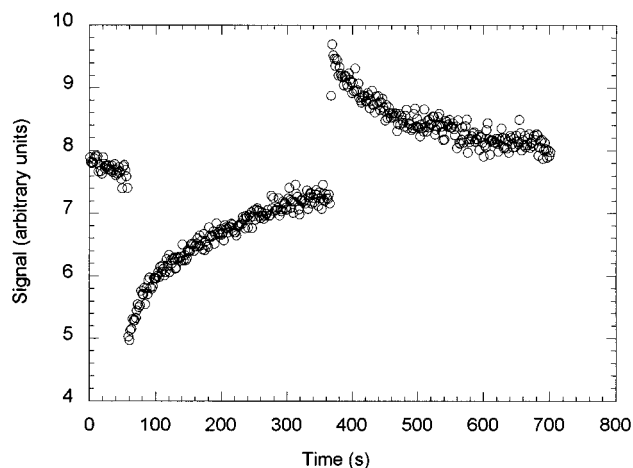


Figure 1. Representative uptake experiment on 65.6% H₂SO₄ at 213 K: HOBr mass spectrometer signal as a function of time.

absorption cell pressures below 150 Torr; at these pressures we saw no evidence for Br₂O contamination.

Results

Solubility of HOBr in Sulfuric Acid. HOBr uptake was measured for acid concentrations from 59.7 to 70.1 wt %, at temperatures ranging from 213 to 238 K. Figure 1 shows a representative uptake experiment on 65.6% H₂SO₄ at 213 K. At 60 s the HOBr signal had reached a steady-state value and the injector was pulled back 8.0 cm over the film. The HOBr signal dropped sharply and slowly recovered to a level close to its initial value. The speed of this recovery varied with composition and temperature. When, at 400 s, the injector was pushed back to its original position, there was a surge in the signal arising from HOBr desorption, followed by a decay to its initial value.

In our earlier work on HOBr uptakes we observed a steady-state loss of HOBr on sulfuric acid films which we attributed to self-reaction because the loss kinetics were observed to be second-order.³ To minimize the possibility of the self-reaction in this study we operated with low partial pressures of HOBr (P^{HOBr} well below 3 × 10⁻⁹ atm). Under these conditions we saw no evidence for a steady-state loss of HOBr in sulfuric acid. Large uptakes did sometimes result in very slow recovery of the gas-phase HOBr, upon exposure to the sulfuric acid film, but none of our uptake curves showed evidence of time-independent uptake in the form of a positive *y*-intercept in a $\gamma(t)$ versus $t^{-1/2}$ plot (see Figure 2, for example). Since HOBr partial pressure influences the direction of the equilibrium in (R7) it thus seems likely that the second-order kinetics observed in our previous work may well have arisen from HOBr reacting with itself under the substantially higher HOBr partial pressures used.

With such low HOBr partial pressures, it is clear from Figure 1 that the mass spectrometer signal for these experiments was quite noisy. As a result, the results of several measurements were averaged to give each data point in Figure 3 and Table 1. All the data are from uptakes measured on fresh sulfuric acid surfaces. In addition, we used only the early-time time data from each uptake measurement to determine the value of $HD^{1/2}$, to make the measurements less sensitive to changing HOBr baselines. Although we interpolated linearly between starting and final HOBr baselines to obtain a baseline appropriate for the time-dependent uptake coefficient calculations, the uncertainties are minimized by using only the first one to two minutes

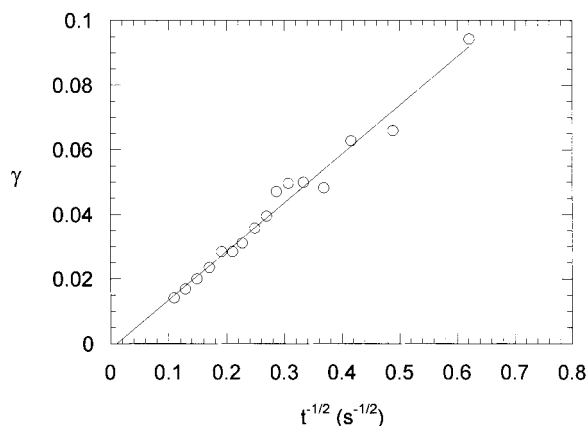


Figure 2. Time-dependent uptake coefficient, $\gamma^{\text{HOBr}}(t)$, plotted versus $1/t^{1/2}$ for the data in Figure 1.

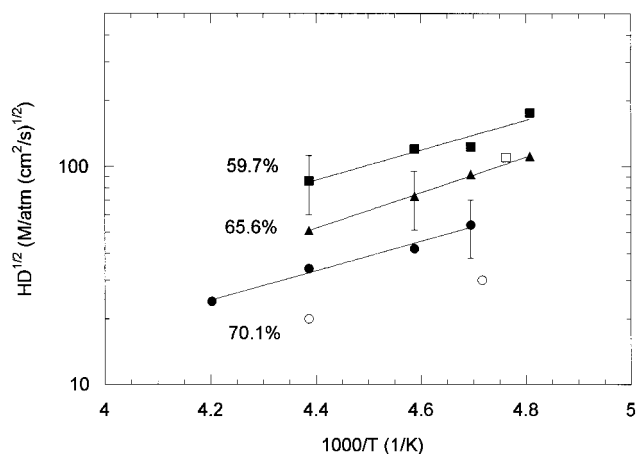


Figure 3. Temperature dependence of $HD^{1/2}$ at 59.7 (squares), 65.6 (triangles), and 70.1 (circles) wt %. Each point is the average of several measurements over different days. Open circles: data from Abbatt.² Open square: data from Hanson and Ravishankara.²

TABLE 1: $HD^{1/2}$ for HOBr in Sulfuric Acid Solutions

H ₂ SO ₄ (%)	T (K)	$HD^{1/2}$ (M atm ⁻¹ cm s ^{-1/2})	H (M atm ⁻¹)
59.7	208	176	1.2×10^6
59.7	213	123	6.3×10^5
59.7	218	120	4.7×10^5
59.7	228	86	2.2×10^5
65.8	208	111	1.2×10^6
65.8	213	92	7.1×10^5
65.8	218	73	4.1×10^5
65.8	228	51	1.7×10^5
70.1	213	54	6.5×10^5
70.1	218	42	3.5×10^5
70.1	228	34	1.6×10^5
70.1	238	24	7.1×10^4

of data. To justify this approach we performed a systematic comparison between the early time data (defined as up to 20 s after the injector was pulled back) and the late time data (from 20 s to the point where the injector was pushed back in). Agreement between the values of $HD^{1/2}$ derived from the early and late data was always within the precision uncertainties of the reported results ($\pm 30\%$). Nevertheless, when the experiments with the largest uptakes were analyzed, there was a small discrepancy between the two with the early data giving slopes up to 25% smaller. As a result the following systematic uncertainties are assigned to $HD^{1/2}$: $\pm 15\%$ for values below 50 M/atm(cm²/s)^{1/2}, $\pm 30\%$ for values close to 100 M/atm(cm²/s)^{1/2}, and $\pm 40\%$ for values around 150 M/atm(cm²/s)^{1/2}. These uncertainties are somewhat difficult to estimate, but they attempt

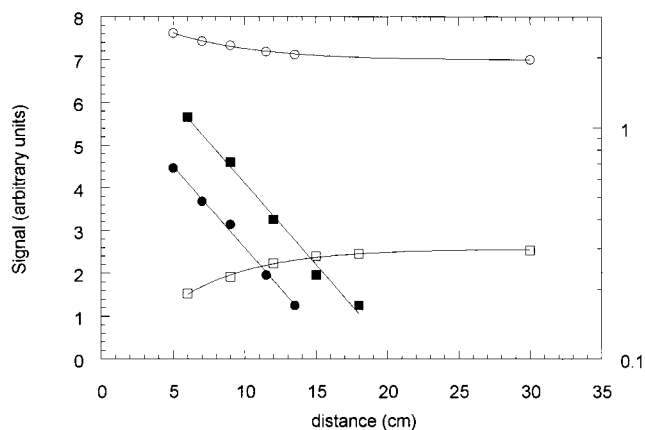


Figure 4. A comparison of HCl decay (circles) and BrCl growth (squares) on 70.1 wt % H₂SO₄ at 228 K. Open symbols represent observed mass spectrometer signals (left axis) and closed symbols represent the effective decays, after backgrounds have been subtracted (right axis).

to take into account the linearity of the γ vs $(1/t)^{1/2}$ plots and the uncertainties in measuring the uptake coefficients.

As shown in the Figure, the values of $HD^{1/2}$ are within a factor of 2 of our previous measurements and that of Hanson and Ravishankara.^{2,3} Although the disagreement lies just within the estimated uncertainties, the older data appear to be systematically lower than the results from this work. The discrepancy between our two sets of data may result from the substantially higher partial pressures used in the earlier study. In particular, we observed that there was an inverse dependence of the measured values of $HD^{1/2}$ on P^{HOBr} for pressures above 3×10^{-9} atm, and no dependence for the data at much lower partial pressures that are reported in Figure 3. This dependence at high partial pressures could possibly arise via the formation of small, undetectable amounts of Br₂O formed in the HOBr self-reaction occurring before the injector flow reached the sulfuric acid film. The Br₂O would then react on the film to reform HOBr, and lower the apparent uptake. In experiments where we knew Br₂O was present in the source, we indeed saw formation of HOBr when the source flow was exposed to the acid film.

Also, it should be noted that uptakes measured on films which had previously been exposed to HOBr were at times smaller, by up to a factor of 2, than those measured on fresh surfaces. We do not know the reason for this erratic behavior, which was not observed in earlier studies,³ and we have only reported measurements of $HD^{1/2}$ performed on previously unexposed surfaces as a result.

Reaction of HOBr with HCl in Sulfuric Acid Solutions.

We first tried to measure the first-order loss of HOBr due to reaction with excess HCl in sulfuric acid, but because the solubility of HOBr is so much greater than that of HCl at these sulfuric acid concentrations, we were unable to put enough HCl in the gas phase to achieve pseudo first-order loss rates with HOBr as the limiting reagent. The obvious solution to this problem was to measure the first-order loss of HCl instead, with HOBr in excess. Figure 4 shows a comparison of first-order HCl decay and BrCl growth curves for one experiment conducted in that mode. Reaction probabilities calculated from these curves agree within 10%, well within the variability of the individual measurements. Due to the HCl background in our detector, it was generally more convenient in these experiments to monitor the growth of BrCl.

Figure 5 plots measured γ^{HCl} versus P^{HOBr} for sulfuric acid compositions 59.7, 65.6, and 70.1 wt % at temperatures ranging

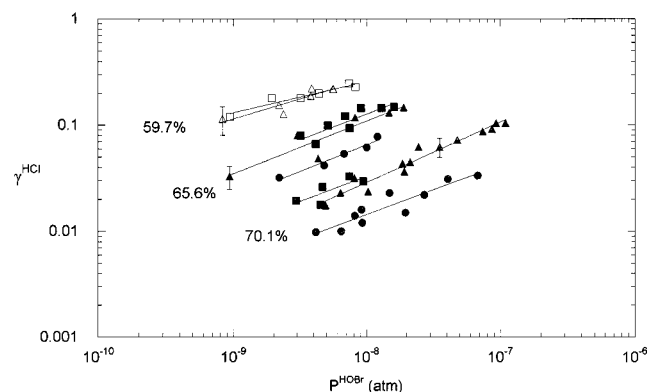


Figure 5. A log–log plot of γ^{HCl} versus P^{HOBr} for sulfuric acid compositions 59.7, 65.6, and 70.1 wt % at 213 K (squares), 228 K (triangles), and 238 K (circles).

from 213 to 238 K. A log–log plot gives slopes ranging from 0.47 to 0.57 for H_2SO_4 compositions 65.6 and 70.1 wt %. At these compositions, γ^{HCl} is sufficiently small that the data are well-described by (E5). The slopes for the data at 59.7 wt % are significantly smaller (~ 0.3), as expected for large values of γ^{HCl} , and these data are better described by (E4). Each point in Figure 5 is the average of several measurements taken on the same sulfuric acid film under constant conditions. The error bars are an indication of the variability of the individual measurements and the errors arising from the gas-phase diffusion correction.

In general, a number of growth profiles were measured on the same film at roughly the same HOBr flow rate. Profiles at early times were discarded if the HOBr signal had not stabilized, indicating that the film was not fully saturated with HOBr. Similarly, we did not use runs from the end of a run if they were substantially different from early runs. In this case we were concerned that the composition of the sulfuric acid film may have changed somewhat. We should also note that the HCl partial pressure had a tendency to slowly drift upward during the course of a run, probably due to a slow conditioning of the lines connecting the HCl reservoir to the flow tube. This increase was not fast enough to affect an individual decay. However, at low values of $[\text{HOBr}]_i/[\text{HCl}]_i$, the system could be pushed out of the pseudo first-order regime, resulting in artificially low values of γ^{HCl} . These values were discarded and the measurements were retaken at a reduced P^{HCl} .

The low conversion efficiency of our HOBr source means that a substantial amount of Br_2 was also introduced into the reaction tube. To ensure that a reaction involving Br_2 was not also producing BrCl and so affecting the BrCl growth curves, we directed the Br_2 and water vapor through a bypass valve around the HgO tube, thereby introducing Br_2 and water, but no HOBr into the upstream end of the reaction tube. Exposing HCl to the sulfuric acid films under these conditions produced no BrCl.

Note that the potential complications caused by Br_2O in the reversible uptake experiments do not arise in the kinetics experiments, since the HOBr flow is introduced upstream of the sulfuric acid film. Any residual Br_2O from the HOBr source, which might be converted to HOBr upon entering the reaction tube, would contribute to the overall P^{HOBr} monitored with the mass spectrometer. Also, although one might expect substantial amounts of Br_2O present in the flow tube based simply on the partial pressure of HOBr and thermodynamic considerations,¹⁶ we saw no evidence for the reverse reaction, conversion of

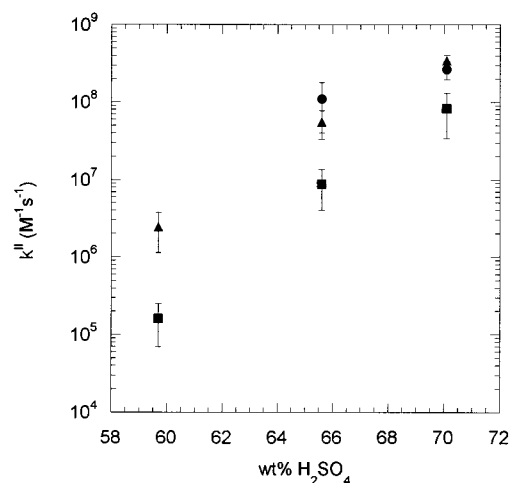


Figure 6. Composition dependence of the second-order reaction rate coefficient for the reaction $\text{HOBr} + \text{HCl} \rightarrow \text{BrCl} + \text{H}_2\text{O}$, at 213 K (squares), 228 K (triangles), and 238 K (circles).

TABLE 2: Liquid-Phase Rate Constants for HOBr/HCl in Sulfuric Acid Solutions

H_2SO_4 (%)	T (K)	H^{HCl} (M atm^{-1})	D^{HCl} ($\text{cm}^2 \text{s}^{-1}$)	H^{HOBr} (M atm^{-1})	k^{II} ($\text{M}^{-1} \text{s}^{-1}$) ^a
59.7	213	2.74×10^4	4.91×10^{-8}	6.89×10^5	$(1.6 \pm 0.9) \times 10^5$
59.7	228	6.37×10^3	1.99×10^{-7}	1.72×10^5	$(2.4 \pm 1.3) \times 10^6$
65.6	213	1.94×10^3	2.16×10^{-8}	6.89×10^5	$(8.7 \pm 4.8) \times 10^6$
65.6	228	5.28×10^2	1.10×10^{-7}	1.72×10^5	$(5.5 \pm 2.2) \times 10^7$
65.6	238	2.37×10^2	2.41×10^{-7}	7.48×10^4	$(1.05 \pm 0.70) \times 10^8$
70.1	213	2.61×10^2	8.75×10^{-9}	6.89×10^5	$(8.3 \pm 4.9) \times 10^7$
70.1	228	8.05×10^1	5.93×10^{-8}	1.72×10^5	$(3.4 \pm 0.6) \times 10^8$
70.1	238	3.91×10^1	1.46×10^{-7}	7.48×10^4	$(2.7 \pm 0.7) \times 10^8$

^a Uncertainties are 1- σ precisions.

HOBr to Br_2O . Perhaps this is because the kinetics of that process are slower than the heterogeneous conversion of Br_2O to HOBr.

To extract the second-order rate constant, k^{II} , for (R2), we fit the uptake coefficient data to (E4), with the value of the mass accommodation coefficient set to unity.¹⁴ Figure 6 shows k^{II} plotted versus sulfuric acid composition. Values for the parameters H^{HCl} (ref 17), D^{HCl} (ref 18), and H^{HOBr} used to calculate the rate constants are listed in Table 2. Error estimates given in the Figure and Table are 1- σ precisions, determined by the uncertainties in the uptake coefficients (20 to 35%) and the scatter about the lines-of-best-fit. The overall uncertainties in the rate constants are difficult to estimate accurately, but they are considerably larger (approximately +200/–75%), arising from the precision error and from the uncertainties in the values of $H^{\text{HCl}}(\pm 50\%)$, $H^{\text{HOBr}}(\pm 50\%)$, $D^{\text{HCl}}(\pm 20\%)$, and $P^{\text{HOBr}}(\pm 20\%)$.

Discussion

HOBr Solubility in Sulfuric Acid Solutions. Henry's law coefficients were determined from the measured values of $HD^{1/2}$ using liquid-phase diffusion constants calculated using ref 18 (see Table 1). Figure 7 plots H as a function of inverse temperature. Although there is a clear Clausius–Clapeyron-like temperature dependence, H shows essentially no dependence on composition. Uptake measurements of HOCl by Donaldson et al. show a similar trend in solubility in sulfuric acid solutions at acid concentrations greater than 60%.¹⁹ Under a physical model of solubility, HOBr solubility is predicted to decrease with increasing acid concentration.²⁰ Thus, it is possible that the enhancement of the solubility of HOBr at high acid concentra-

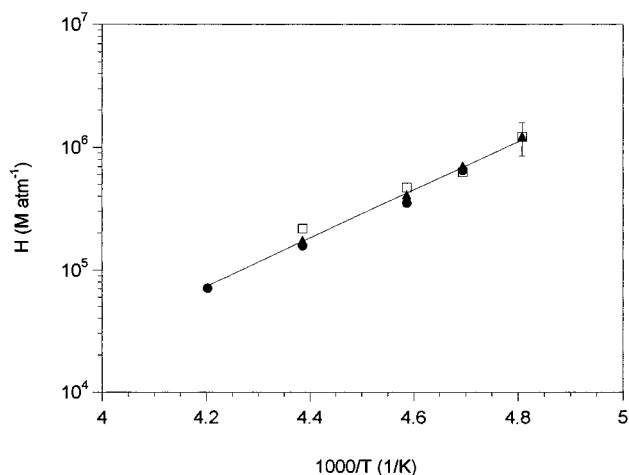


Figure 7. Temperature dependence of the Henry's law constant for HOBr in 59.7 (squares), 65.6 (triangles), and 70.1 (circles) wt % H₂SO₄.

tion is due to an increasing degree of protonation, which closely matches the decrease in solubility due to physical processes:



A simple functional form fits the data nicely:

$$H^{\text{HOBr}} = (4.6 \pm 10) \times 10^{-4} \exp((4.50 \pm 0.48) \times 10^3/T) \quad (\text{E7})$$

where T is in Kelvin, H is in units of M/atm and the uncertainties are at the 1- σ level. The temperature dependence gives a heat of dissolution of HOBr in sulfuric acid solutions of -9 ± 1 kcal/mol.

Reaction of HOBr with HCl in Sulfuric Acid Solutions.

Figure 6 shows the strong dependence of the second-order reaction rate coefficient on acid concentration. At 213 and 228 K, k^{II} increases by over 2 orders of magnitude as the sulfuric acid concentration increases from 59.7 to 70.1 wt %, whereas the 238 K data show a somewhat weaker dependence. Donaldson and co-workers noted a similar, though weaker, composition dependence in their studies of the related reaction, $\text{HOCl} + \text{HCl} \rightarrow \text{Cl}_2 + \text{H}_2\text{O}$, and proposed that it stems from an ionic reaction mechanism.¹⁹ As they discuss, the most likely ionic mechanism involves protonation of HOBr followed by reaction with Cl^- :



Assuming a rapid equilibrium in (R9), as might be expected to occur in strongly acidic solutions, then the rate of the overall reaction can be expressed as

$$\text{Rate} = k_{10}K_9[\text{HOBr}][\text{H}^+][\text{Cl}^-] \quad (\text{E8})$$

where K_9 is the equilibrium constant for (R9). The second-order rate constant for the overall reaction

$$k^{\text{II}} = k_{10}K_9[\text{H}^+] \quad (\text{E9})$$

is qualitatively consistent with our observed dependence on acid concentration. The large changes in the measured rate constants with only relatively small changes in the weight percent composition of the solutions may be related to the much higher

effective acidity of a 70 wt % solution compared to a 60% solution, a concept treated in detail by Donaldson et al.¹⁹

An alternative mechanism valid at low acid concentrations, involves initial attack by Cl^- on HOBr:²¹



For very low acid concentrations, (R12) would be rate-limiting and the overall rate expression would be

$$\text{rate} = k_{12}K_{11}[\text{HOBr}][\text{H}^+][\text{Cl}^-] \quad (\text{E10})$$

also implying a direct dependence on acid concentration. However, for high acid concentrations, and a diffusion-limited k_{12} , k_{11} may be equal to or even much less than $k_{12}[\text{H}^+]$. In this case, k^{II} would approach the limiting value, $k^{\text{II}} \approx k_{11}$, and there would be no acid dependence. At this point we are not able to discriminate between the two mechanisms outlined above, nor determine whether the reaction instead proceeds as a single, concerted process.

It is also of interest to consider the factors which are controlling the absolute magnitude of the rate constants and their temperature dependence. First, the rate constants measured with the 70.1% acid solutions are similar to, but somewhat larger than, those calculated for a diffusion-controlled reaction, assuming neutral reagents.²² In particular, assuming an effective collision diameter of 10^{-7} cm, the measured rate constants are factors of 7, 4, and 1.5 larger than the calculated diffusion-controlled rate constants for 213, 228, and 238 K, respectively. Given that this collision diameter is an estimate and may well be considerably larger if significant solvation of the reactant ions is occurring,²³ that diffusion-controlled rate constants between ions can be several times larger than those between neutral species,²² and the relatively large experimental uncertainties, we feel reasonably confident that the rate constants measured in the 70.1 wt % solutions are under diffusion-control and that an experimental error has not been made. It is also worth pointing out that the discrepancy could arise from uncertainties in the values of H^{HCl} , for 70 wt % solutions.

For a diffusion-controlled reaction, one would expect the apparent activation energy in the 70.1 wt % rate constants, arising from the temperature dependence of the diffusion coefficients, to be on the order of 11 kcal/mol. This is similar to the activation energy which is exhibited between the 213 and 228 K rate constants: 9.2 kcal/mol. However, one would expect the 238 K rate constant to be somewhat larger than that at 228 K, and the reason that it is not may arise simply from overall experimental uncertainties, which are roughly +200/-75% for each point. If the 238 K rate constant is indeed a factor of 2 to 3 too low, then this would also explain the differing dependence on acidity between the 238 K data and the 228 and 213 K data.

The activation energy exhibited by the 65.6 wt % solution data, 10.2 kcal/mol, is also similar to that which one would calculate for a diffusion-controlled reaction, 9.8 kcal/mol, even though the reaction is very clearly not under diffusion control. For the protonation mechanism the overall rate constant governing this reaction is given by (E9). Thus, one scenario which would lead to a diffusion-controlled temperature dependence is if (R10) is a diffusion-limited reaction (as expected, for a process involving an anion and cation) and if there is only a minor temperature dependence arising from the equilibrium constant K_9 .

Finally, it is important to point out that our previously published liquid-phase rate constant for this reaction is likely to be in error.³ In the early experiments, HOBr decays were analyzed in the presence of HCl, and it was assumed that since HCl was in excess in the gas phase it would also be in excess in the solution. From the solubilities of HOBr and HCl, it can now be readily shown that that was not true under the experimental operating conditions. A manifestation of these conditions was the relatively poor quality of the plot of the γ^{HOBr} vs $(P^{\text{HCl}})^{1/2}$ in ref 3 (Figure 11). There is good agreement between our present data and the rate constant of Hanson and Ravishankara in 60% solution at 210 K.²

Atmospheric Implications. As mentioned in the Introduction, (R2) proceeding on sulfuric acid aerosols is an activation mechanism for HCl in the atmosphere, one which may potentially compete with gas-phase loss via reaction with OH and with other heterogeneous processes. The extremely high solubility of HOBr in acid solutions and the magnitude of the liquid-phase rate constant enhance the overall rate of this process despite the low atmospheric abundance of gas-phase HOBr.

To make a quantitative assessment of the rate of HCl activation we use fundamental physical parameters measured both in this work and elsewhere. Specifically, we calculate lifetimes for heterogeneous HCl loss in both the lower stratosphere and tropospheric boundary layer using

$$\text{rate of HCl loss} = [\text{HOBr}]_{\text{atm}} \gamma^{\text{HOBr}} cA/4 \quad (\text{E11})$$

when HCl is in excess in the liquid phase, and

$$\text{rate of HCl loss} = [\text{HCl}]_{\text{atm}} \gamma^{\text{HCl}} cA/4 \quad (\text{E12})$$

when HOBr is in excess. For these equations, $[\text{HOBr}]_{\text{atm}}$ and $[\text{HCl}]_{\text{atm}}$ are the concentrations of HOBr and HCl under atmospheric conditions, and A is the total aerosol surface area. The uptake coefficients used in these equations are those appropriate for atmospheric conditions. That is, following the approach described in detail in ref 24, they have been calculated from (E3), which has been corrected to take into account the fact that the reaction is not occurring in a thick film but rather in a particle of radius a :

$$\gamma = 4RTH(Dk^{\text{I}})^{1/2} [\coth a/l - l/a] \quad (\text{E13})$$

where l is the reacto-diffusive depth

$$l = (D/k^{\text{I}})^{1/2} \quad (\text{E14})$$

To assess the rate of HCl activation over a wide range of atmospheric conditions requires that each of the fundamental physical parameters in (E13) and (E14) be parametrized in terms of typical atmospheric ambient conditions. Specifically, for both the stratospheric and tropospheric calculations presented below we determine the sulfuric acid aerosol compositions from an assumed water vapor partial pressure at a specific temperature.²⁵ The various physical terms, such as the solubilities, diffusivities, and rate constants, are then parametrized in terms of the temperature and acid composition.

Stratospheric Conditions. Just as it is important to determine which reactant is in excess in the sulfuric acid solutions in our experiments, it is also necessary to do so for sulfate aerosols in the atmosphere. The solubility of HCl in sulfuric acid is described as a function of both temperature and aerosol composition by the model of Carslaw et al., which has been tuned to match a range of experimental measurements.¹⁷ As described in the Discussion, the solubility of HOBr is derived

from the values of $\text{HD}^{1/2}$ measured in this work. When these solubilities are taken into consideration for temperatures and acid compositions encountered in the lower stratosphere, it is calculated that the ratio of the concentration of HOBr to that of HCl dissolved in sulfuric acid aerosols is larger than unity for all temperatures greater than 204 K at 20 km altitude, assuming partial pressures of 5.9×10^{-13} atm for HOBr (i.e., 10 pptv, a typical night-time value), 5.9×10^{-11} atm (i.e., 1 ppbv) for HCl, and 3.0×10^{-7} atm for H_2O (i.e., 3.0×10^{-4} mbar). Clearly this ratio will be smaller if less HOBr is present, as during the day, when it is efficiently photolyzed. Thus, for relatively warm conditions, the reaction is most accurately modeled with HOBr in excess throughout the aerosols and with HCl as the limiting reagent. For temperatures less than 204 K, where the ratio of dissolved HOBr to HCl is less than one, the reverse is true and HOBr will be the limiting reagent. Note that the exact crossover temperature where one reactant moves from existing in excess to being the limiting reagent is dependent upon the assumed value for the water vapor mixing ratio and, of course, the partial pressures of HCl and HOBr.

The remaining parameters to be expressed in (E13) are the liquid-phase diffusion coefficient for HCl, which is calculated from ref 18, and the second-order, liquid-phase rate constant, which is taken from our measurements. Specifically, to arrive at an expression for k^{II} as a function of both temperature and acid composition, we have determined both the dependence of k^{II} on composition at a fixed temperature and its dependence on temperature at a fixed acid composition for the 213 and 228 K data sets, i.e., those which are closest in temperature to stratospheric conditions. By so doing, we arrive at the following expression:

$$k^{\text{II}} = \exp(0.542C - 6.44 \times 10^3/T + 10.3) \quad (\text{E15})$$

where C is the acid composition in wt %, T is in Kelvin, and k^{II} is in $\text{M}^{-1} \text{s}^{-1}$. The rate constants calculated with this expression agree with the experimentally derived values to within $\pm 40\%$, i.e., well within the experimental uncertainties, for all acid compositions at 213 and 228 K.

With the above parametrizations we can calculate the reactive uptake coefficients for (R2) under a set of typical atmospheric conditions. First, for relatively warm conditions where HCl is the limiting reagent, HCl uptake coefficients are shown in Table 3. Note the calculations have been performed with both 0.2×10^{-4} cm radius aerosols, typical of background aerosol conditions, and with "volcanic" aerosols of 0.5×10^{-4} cm radius. Gas-phase mixing ratios are 10 pptv HOBr and 5.0 ppmv water vapor, and the altitude is 20 km. For temperatures less than 204 K, HOBr is the limiting reagent and appropriate uptake coefficients are also listed in the table, assuming 1 ppbv HCl.

For these uptake coefficients, HCl activation rates are given in Table 4 for three scenarios. First, the loss rate of HCl via the HOBr/HCl heterogeneous reaction on sulfate aerosols is tabulated, using (E11) and (E12), under both volcanically quiescent conditions ($A = 1.0 \times 10^{-8} \text{ cm}^2/\text{cm}^3$) and for aerosol conditions prevalent soon after the Mt. Pinatubo volcanic eruption ($A = 2.0 \times 10^{-7} \text{ cm}^2/\text{cm}^3$). Also, the activation rate via the gas-phase process (R13)



is shown, assuming $[\text{OH}] = 1.0 \times 10^6 \text{ molecules/cm}^3$ and the JPL rate constant.²⁶

Acknowledging that the comparison of HCl activation rates for (R2) and (R13) is most accurately performed using a

TABLE 3: Uptake Coefficients Due to the HOBr/HCl Reaction under Lower Stratospheric Conditions (see text)

<i>T</i> (K)	H ₂ SO ₄ (%)	<i>H</i> ^{HOBr} (M/atm)	<i>H</i> ^{HCl} (M/atm)	<i>k</i> ^{II} (M ⁻¹ s ⁻¹)	reagent ratio ^a	<i>a</i> = 0.2 × 10 ⁻⁴ (cm)		<i>a</i> = 0.5 × 10 ⁻⁴ (cm)	
						<i>γ</i> ^{HOBr}	<i>γ</i> ^{HCl}	<i>γ</i> ^{HOBr}	<i>γ</i> ^{HCl}
218	72.7	4.2 × 10 ⁵	5.0 × 10 ¹	5.7 × 10 ⁸	8.4 × 10 ¹		7.1 × 10 ⁻⁵		1.0 × 10 ⁻⁴
214	70.2	6.2 × 10 ⁵	2.3 × 10 ²	8.5 × 10 ⁷	2.7 × 10 ¹		9.0 × 10 ⁻⁵		1.7 × 10 ⁻⁴
210	67.5	9.3 × 10 ⁵	1.2 × 10 ³	1.1 × 10 ⁷	7.8		9.3 × 10 ⁻⁵		2.1 × 10 ⁻⁴
206	64.2	1.4 × 10 ⁶	7.7 × 10 ³	1.0 × 10 ⁶	1.8		8.5 × 10 ⁻⁵		2.1 × 10 ⁻⁴
202	60.3	2.2 × 10 ⁶	6.7 × 10 ⁴	6.6 × 10 ⁴	3.3 × 10 ⁻¹	1.1 × 10 ⁻²		2.9 × 10 ⁻²	
198	55.3	3.4 × 10 ⁶	9.1 × 10 ⁵	2.3 × 10 ³	3.8 × 10 ⁻²	8.9 × 10 ⁻³		2.2 × 10 ⁻²	

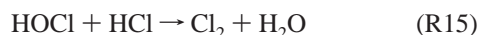
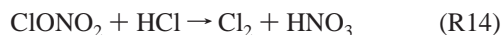
^a Reagent ratio = ratio of HOBr to HCl dissolved in sulfuric acid aerosol, assuming partial pressures given in text.

TABLE 4: HCl Activation Rates by HOBr/HCl Reaction and by Gas-Phase Reaction with OH under Lower Stratospheric Conditions (see text)

<i>T</i> (K)	Rates of HCl Activation (molecules cm ⁻³ s ⁻¹)		
	background aerosol ^a	volcanic aerosol ^b	gas phase ^c
218	13	3.7 × 10 ²	1.0 × 10 ³
214	16	6.0 × 10 ²	1.0 × 10 ³
210	16	7.6 × 10 ²	1.0 × 10 ³
206	16	7.6 × 10 ²	1.0 × 10 ³
202	13	6.5 × 10 ²	9.8 × 10 ²
198	10	5.0 × 10 ²	9.7 × 10 ²

a: *a* = 0.2 × 10⁻⁴ cm, A = 1 × 10⁻⁸ cm²/cm³ b: *a* = 0.5 × 10⁻⁴ cm, A = 2 × 10⁻⁷ cm²/cm³ c: [OH] = 1.0 × 10⁶ molecules/cm³

photochemical model which incorporates the diurnal dependence of the concentrations of HOBr and OH, the potential significance of the rate of heterogeneous HCl activation under volcanic aerosol conditions is nevertheless clearly illustrated in Table 4. It is now well-known that other heterogeneous reactions, such as



are efficient activators of HCl at temperatures below about 205 K, where the solubility of HCl becomes high.²⁴ However these reactions are not very efficient at higher temperatures, where the sulfate aerosols become more concentrated and the solubilities of HCl are significantly reduced. By contrast, the ability of (R2) to activate HCl is significant relative to gas-phase processes at significantly higher temperatures, temperatures which are frequently encountered at mid-latitudes in the lower stratosphere.

Two points should be made concerning these conclusions. First, the reason for the relatively weak temperature dependence of the HCl uptake coefficient via (R2) (see Table 3) is due to offsetting factors: as the temperature rises, the solubilities of HCl and HOBr decrease but the second-order rate constant increases. It is also important to note that the estimates of the efficiency of (R2) as an HCl-activating process are particularly sensitive to the rate constant measured in 70 wt % solutions at 213 K. As mentioned above, that rate constant is larger than that one calculates for a diffusion-controlled reaction involving neutral species. If the rate constant turns out to be erroneously high, perhaps due to uncertainties in the value of *H*^{HCl} used in the data analysis or for some other reason, then the implications of this work will have to be adjusted accordingly.

Tropospheric Conditions. Using our experimental data we can make an estimate of the rate of HCl activation via (R2) which may occur under the conditions prevalent in the high Arctic boundary layer during springtime. Although these calculations are subject to considerable uncertainties, it should be noted that the goal here is to determine the potential

importance of this chemistry to the marine boundary layer rather than to perform a definitive calculation. To be specific, the HCl-lifetime calculation is subject to uncertainties arising from the variable nature of the relative humidity, temperature and aerosol composition in the boundary layer, estimates of the gas-phase concentrations of HOBr and HCl, and the fact that the HOBr solubility and the liquid-phase rate constants have been measured in acid solutions closer in composition to those prevalent in the stratosphere than in the troposphere.

To be consistent with a previous publication where we evaluated the rate of the HOCl/HBr heterogeneous reaction assuming 40 wt % sulfuric acid aerosols at 233 K,⁷ we will do the same in this work. This acid composition is similar to that which would be in equilibrium with the average relative humidity of 83% measured by Stabler et al. for conditions during a recent Polar Sunrise Experiment.²⁷ For these conditions, it is straightforward to determine the solubility of HCl in the aerosols, using the model of Carslaw et al.¹⁷ For *H*^{HOBr}, we continue to assume that there is no dependence upon the acid composition, as we have shown to be valid for solutions from 60 to 70 wt %. If there is indeed an acid dependence for less acidic solutions and the system behaves in a manner similar to HOCl dissolved in sulfuric acid,²⁰ then the true Henry's Law constant will be larger than the value we have assumed here and the HCl processing rates will be correspondingly faster. For these assumptions, HCl will be in excess over HOBr in solution, assuming 0.5 ppbv HCl and 10 pptv HOBr in the boundary layer.^{1,6}

Large uncertainties clearly arise when trying to estimate the value of the liquid-phase rate constant at 233 K for 40 wt % solutions using the experimental data from Figure 6. In particular, for the two temperatures closest to tropospheric conditions, the 238 K data are very much less dependent upon acid composition than the 228 K data. Thus, the approach we take here is to calculate the HOBr uptake coefficient for a range of rate constants which are at least consistent with our data set. In particular, we have performed the calculations using two values, ranging from 10⁵ M⁻¹ s⁻¹, a value more consistent with the 238 K data, to 10² M⁻¹ s⁻¹, consistent with the 228 K data. When we do so, the HOBr uptake coefficients which are calculated, assuming 0.15 μm aerosol radius,²⁷ are given in Table 5. The corresponding HCl activation rates via (R2) and via gas-phase reaction with 10⁶ molecules/cm³ of OH are also given in Table 5, assuming an aerosol surface area of 6 × 10⁻⁷ cm²/cm³^{4,27} and HOBr mixing ratios of 10 pptv.⁶

The point to be made from the results in Table 5 is that there is the distinct possibility that high levels of active bromine will activate HCl within the Arctic boundary layer. As in the stratosphere, a small but significant fraction of gas-phase HCl and HOBr will be partitioned to the aerosol when the temperatures are low and the aerosol particles become dilute. Heterogeneous HCl activation rates can then compete with, or overwhelm, gas-phase processes. The degree to which this

TABLE 5: HCl Activation Rates by HOBr/HCl Reaction and by Gas-Phase Reaction under Arctic Boundary Layer Conditions (see text)

$k^{\text{II}} (\text{M}^{-1} \text{s}^{-1})$	γ^{HOBr}	rate of HCl activation (molecules $\text{cm}^{-3} \text{s}^{-1}$) ^a
10^2	2.8×10^{-4}	2.9×10^2
10^5	2.2×10^{-1}	2.3×10^5
gas-phase reaction with OH (R13)		9.1×10^3

^a $a = 1.5 \times 10^{-5} \text{ cm}$, $A = 6 \times 10^{-7} \text{ cm}^2/\text{cm}^3$, $[\text{OH}] = 1 \times 10^6 \text{ molecules/cm}^3$.

suggestion is accurate is very much dependent upon the value of the liquid-phase rate constant, which is poorly constrained by the present work. This underscores the need to further pursue the kinetics of (R2) under tropospheric conditions. It can be noted that in an earlier publication, we made similar conclusions with respect to the importance of the HOCl/HBr heterogeneous reaction.⁷ In particular, on the basis of preliminary laboratory studies it was shown that the HOCl/HBr reaction could be important as an HBr activating process, in addition to the previously suggested HOBr/HBr reaction.⁶ Given that both photochemically active bromine and chlorine have been observed in the springtime Arctic makes the extent to which these two halogen families are chemically coupled of considerable interest.⁵

Acknowledgment. This work was funded by the Atmospheric Chemistry Program at the National Science Foundation.

References and Notes

- (1) *Composition, Chemistry and Climate of the Atmosphere*; Singh, H. B. Ed.; Van Nostrand Reinhold: New York, 1995.
- (2) Hanson, D. R.; Ravishankara, A. R. *Geophys. Res. Lett.* **1995**, *22*, 385.
- (3) Abbatt, J. P. D. *J. Geophys. Res.* **1995**, *100*, 14,009.
- (4) Barrie, L. A.; den Hartog, G.; Bottenheim, J. W.; Landsberger, S. *J. Atmos. Chem.* **1989**, *9*, 101.
- (5) Impey, G. A.; Shepson, P. B.; Hastie, D. R.; Barrie, L. A.; Anlauf, K. G. *J. Geophys. Res.* **1997**, *102*, 16,005; Jobson, B. T.; Niki, H.; Yokouchi, Y.; Bottenheim, J.; Hopper, F.; Leitch, R. *J. Geophys. Res.* **1994**, *99*, 25,355.
- (6) Fan, S.-M.; Jacob, D. *J. Nature* **1992**, *359*, 522.
- (7) Abbatt, J. P. D.; Nowak, J. B. *J. Phys. Chem.* **1997**, *101* (2), 131.
- (8) Mozurkewich, M. *J. Geophys. Res.* **1995**, *100*, 14,199.
- (9) Vogt, R.; Crutzen, P. J.; Sander, R. *Nature* **1996**, *383*, 327.
- (10) Sander, R.; Crutzen, P. J. *J. Geophys. Res.* **1996**, *101*, 9121.
- (11) Zhang, R.; Wooldridge, P. J.; Abbatt, J. P. D.; Molina, M. J. *J. Phys. Chem.* **1993**, *97* (7), 351.
- (12) Brown, R. L. *J. Res. Natl. Bur. Stand. (U.S.)* **1978**, *83*, 1.
- (13) Dankwerts, P. V. *Gas-Liquid Reactions*; McGraw-Hill: New York, 1970.
- (14) Hanson, D. R.; Lovejoy, E. R. *J. Phys. Chem.* **1996**, *100* (6), 397.
- (15) Barnes, R. J.; Lock, M.; Coleman, J.; Sinha, A. *J. Phys. Chem.* **1996**, *100*, 453.
- (16) Orlando, J. J.; Burkholder, J. B. *J. Phys. Chem.* **1995**, *99*, 1143.
- (17) Carslaw, K. S.; Clegg, S. L.; Brimblecombe, P. *J. Phys. Chem.* **1995**, *99*, 11,557.
- (18) Klassen, J. K.; Hu, Z.; Williams, L. R. *J. Geophys. Res.* **1998**, *103*, 16,197.
- (19) Donaldson, D. J.; Ravishankara, A. R.; Hanson, D. R. *J. Phys. Chem.* **1997**, *101*, 717.
- (20) Huthwelker, T.; Peter, Th.; Luo, B. P.; Clegg, S. L.; Carslaw, K. S.; Brimblecombe, P. *J. Atmos. Chem.* **1995**, *81*, 21.
- (21) Eigen, M.; Kustin, K. *J. Chem. Soc.* **1962**, *84* (1), 355.
- (22) Steinfeld, J. I.; Francisco, J. S.; Hase, W. L. *Chemical Kinetics and Dynamics*; Prentice-Hall: Englewood Cliffs, NJ, 1989.
- (23) Levine, I. N. *Physical Chemistry*; McGraw-Hill: New York, 1978.
- (24) Hanson, D. R.; Ravishankara, A. R.; Solomon, S. *J. Geophys. Res.* **1994**, *99*, 3,615.
- (25) Carslaw, K. S.; Luo, B.; Peter, T. *Geophys. Res. Lett.* **1995**, *22*, 1,877.
- (26) DeMore, W. B.; Sander, S. P.; Golden, D. M.; Hampson, R. F.; Kurylo, M. J.; Howard, C. J.; Ravishankara, A. R.; Kolb, C. E.; Molina, M. J. *Chemical Kinetics and Photochemical Data for Use in Stratospheric Modeling*, Evaluation Number 12, JPL Publication 97-4, Pasadena, 1997.
- (27) Staebler, R. M.; den Hartog, G.; Georgi, B.; Dusterdieck, T. *J. Geophys. Res.* **1994**, *99*, 25,429.